

# Maximizing Mission Utility within Operational Constraints for the SWARM-EX CubeSat Mission

David Fitzpatrick<sup>1</sup> and Evan Bauch<sup>2</sup> University of Colorado Boulder, Boulder, CO 80309

Rohil Agarwal<sup>3</sup>
Franklin W. Olin College of Engineering, Needham, MA 02492

Scott E Palo<sup>4</sup>
University of Colorado Boulder, Boulder, CO 80309

#### I. Nomenclature

ADCS = Attitude Determination & Control System

BCT = Blue Canyon Technologies

BOL = Beginning of Life

CDH = Command & Data Handling

CP = Co-Planar

ConOps = Concept of Operations

CIRBE = Colorado Inner Radiation Belt Experiment

CU = University of Colorado

EOL = End of Life

EPS = Electrical Power System

EIA = Equatorial Ionization Anomaly

ETA = Equatorial Thermospheric Anomaly

FIPEX = Flux-Probe EXperiment

GNSS = Global Navigation Satellite System

GS = Ground Station HD = High-Drag

LASP = Laboratory for Atmospheric and Space Physics

LD = Low-Drag LEO = Low-Earth Orbit LP = Langmuir Probe

NSF = National Science Foundation

OGNC = Orbital Guidance, Navigation, & Control RAAN = Right Ascension of the Ascending Node

REPTile-2 = Relativistic Electron Proton Telescope integrated little experiment-2

SCI = Science
SoC = State of Charge
STK = Systems Tool Kit
SV = Solar-Velocity
SZ = Solar-Zenith

SWARM-EX = Space Weather Atmospheric Reconfigurable EXperiment

UHF = Ultra-High Frequency VBScript = Visual Basic Script

<sup>&</sup>lt;sup>1</sup>Ph.D. Candidate, david.fitzpatrick@colorado.edu, Ann and H.J. Smead Department of Aerospace Engineering Sciences.

<sup>&</sup>lt;sup>2</sup>Ph.D. Candidate, evan.bauch@colorado.edu, Ann and H.J. Smead Department of Aerospace Engineering Sciences.

<sup>&</sup>lt;sup>3</sup>Undergraduate Research Assistant, ragarwal@olin.edu, Olin Satellite + Spectrum Technology & Policy (OSSTP) Group.

<sup>&</sup>lt;sup>4</sup>Victor Charles Schelke Endowed Professor, scott.palo@colorado.edu, Ann and H.J. Smead Department of Aerospace Engineering Sciences.

#### **II. Introduction**

With space more accessible than ever, academic institutions like the University of Colorado (CU) Boulder have exhibited that small satellites can be leveraged for remarkable space missions capable of making significant advances to both scientific and technological fields. Most of CU Boulder's cutting-edge small satellite projects are CubeSats (small, standardized, rectangular satellites with masses below 14 [kg]), such as the National Science Foundation (NSF)-funded Space Weather Atmospheric Reconfigurable Multiscale EXperiment (SWARM-EX). SWARM-EX will launch three 3U CubeSats in a reconfigurable "swarm" to demonstrate autonomous formation flying capabilities and study the spatial and temporal variability of ion-neutral interactions in the equatorial Ionosphere-Thermosphere region. Although the small stature of CubeSats and their standardized deployer options help to lower unit development cost and facilitate launch opportunities, the physical size limits of CubeSats prove to be a double-edged sword vis-à-vis sustaining a stable power state while hosting instruments with high power demands and often strict pointing requirements. For SWARM-EX, this issue is magnified by the mission's ambitious goals; to comply with mission requirements, a SWARM-EX spacecraft is required to concurrently adhere to numerous attitude requirements (Figure 1), including:

- 1) Point the science instruments no more than 30° off ram (the direction of spacecraft motion) when they are operational;
- 2) Point the Global Navigation Satellite System (GNSS) patch antenna no more than 30° off zenith when the spacecraft are separated by < 10 [km]:
- 3) Point the X-Band patch antenna no more than 18° off boresight from the ground station during downlink;
- 4) Maximize the differential ballistic coefficient during differential drag maneuvers; and
- 5) Maximize solar array power generation at all times.

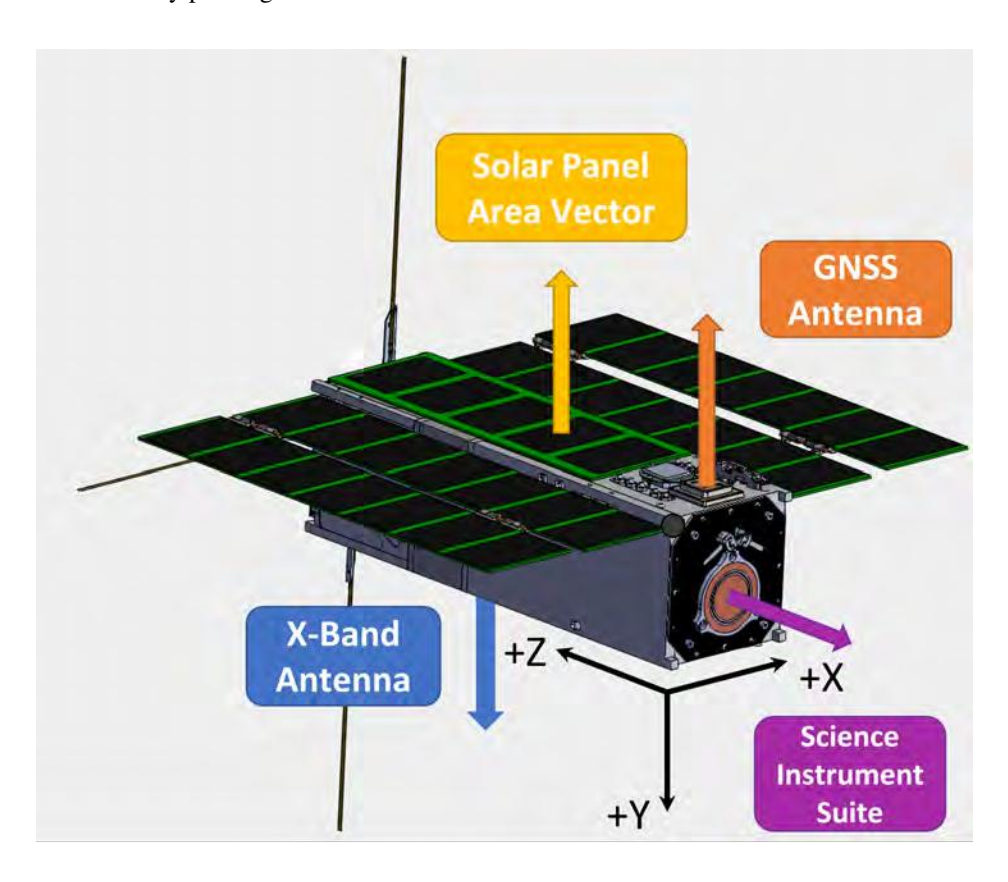


Fig. 1 A rendering of a SWARM-EX CubeSat detailing the science instrument suite, GNSS patch antenna, X-Band patch antenna, and solar panel area pointing vectors alongside the spacecraft body axes.

Consequently, advanced CubeSat missions like SWARM-EX require innovative systems engineering solutions and a complex Concept of Operations (ConOps) to remain "power-positive" during on-orbit operations. Through a combination of intricate pointing profiles, orbital simulations, a comprehensive and coordinated ConOps, battery State of Charge (SoC) simulation tools, and expertise from previous CubeSat missions, the SWARM-EX team has conceived a plan to successfully meet all these mission requirements; it is the aim of the authors to illuminate these strategies as a case study.

## III. SWARM-EX Science and Engineering Objectives

With a nominal launch date in Q4 2023, the SWARM-EX mission is an inter-collegiate CubeSat initiative to launch three identical CubeSats into Low-Earth Orbit (LEO) to investigate advanced scientific phenomena in the upper-atmosphere and demonstrate novel formation flying capabilities. With contributions from Boulder, Stanford University, Georgia Institute of Technology, Western Michigan University, University of Southern Alabama, and Olin College, each CubeSat will be equipped with a low-rate Ultra-High Frequency (UHF) radio, a high-rate X-Band radio (downlink only), and a scalable cold-gas propulsion system to demonstrate the key technologies of on-board autonomy, inter-satellite links, propulsion, and multiuser communications. A Flux-Probe EXperiment (FIPEX) neutral oxygen sensor and Langmuir Probe (LP) measuring ion density will also be onboard to address outstanding questions in aeronomy relevant to the Equatorial Ionization Anomaly (EIA) and the Equatorial Thermospheric Anomaly (ETA).

The primary objectives of the SWARM-EX mission are to (1) better characterize the spatial and temporal variability of the EIA and the ETA and (2) demonstrate cutting-edge engineering technology through autonomous formation flying control algorithms. Flying in a string-of-pearls formation, the SWARM-EX CubeSats will address these objectives by alternating between conducting Science (SCI) experiments and Orbital Guidance, Navigation, & Control (OGNC) experiments, where the former are characterized by much larger mean along-track separations between the spacecraft than the latter (Figure 2).<sup>1</sup>

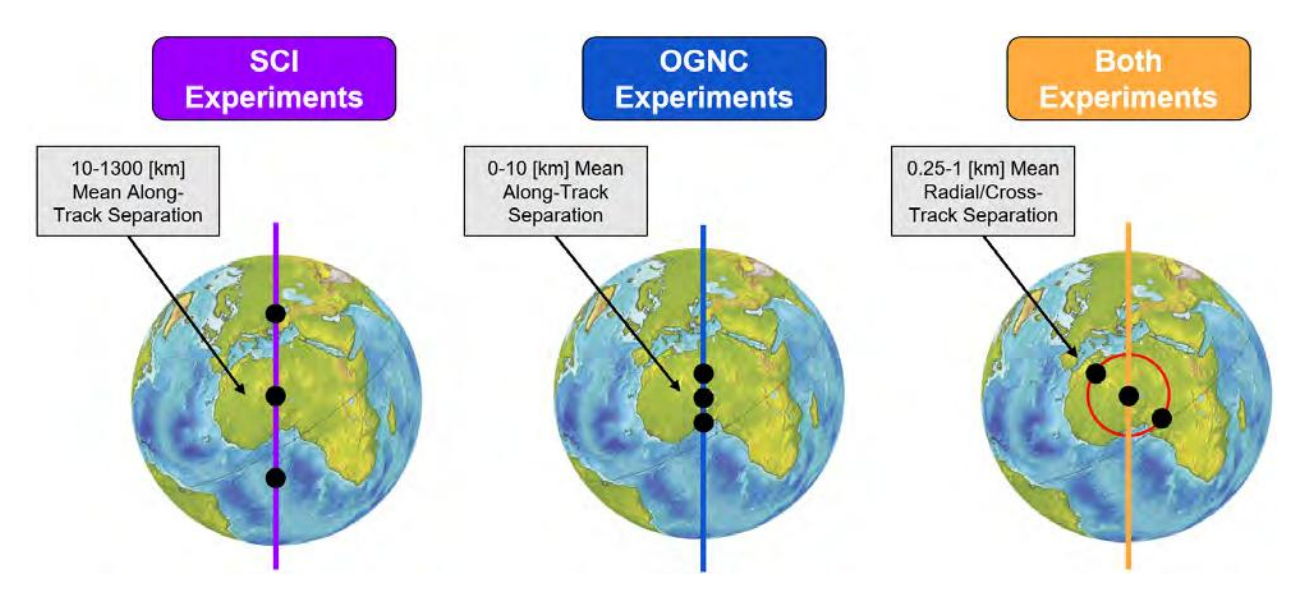


Fig. 2 A visual representation of SWARM-EX's OGNC and SCI experiments detailing their differing ranges of mean along-track separation and string-of-pearls formation.

During SCI experiments, the three CubeSats of SWARM-EX will separate from one another using a combination of onboard propulsion and differential drag to make in-situ measurements of atomic oxygen, the dominant atmospheric component in LEO and the key to better understanding the EIA and ETA. The spacecraft are then brought much closer together during OGNC experiments, where they will further demonstrate fuel balancing through a novel hybrid propulsive/differential-drag control scheme and precise relative orbit determination and prediction. A mean along-track separation of  $\approx 10$  [km] nominally partitions these two experiments.

The cycling of these experiments engenders complex challenges for the SWARM-EX team, particularly with regards to ensuring all spacecraft remain power-positive during the primary mission phases. Preparing effective SCI and OGNC experiments has required the SWARM-EX team to thoroughly plan out the on-orbit operations of SWARM-EX and

<sup>&</sup>lt;sup>1</sup>Both experiments require nonzero mean radial/cross-track separation distances between spacecraft in an effort to considerably mitigate the risk of collisions within the swarm.

craft the comprehensive power analysis delineated below.

# IV. SWARM-EX Operational Orbits and Orbital Timelines

For any CubeSat mission, it is imperative to evaluate the power usage of onboard hardware throughout each stage of the mission. However, due to the many pointing constraints and high-power demands of the science instrument suite, the SWARM-EX team has identified the risk of not maintaining a power-positive state throughout its lifetime as being especially relevant. Consequently, the SWARM-EX team has developed a ConOps that is able to characterize all of the combinations of active onboard hardware that are expected on-orbit to distinguish each associated power-draw state. In this way, the SWARM-EX team can identify portions of the mission where power usage is especially high and, more generally, prepare for the entire mission in terms of power.

The SWARM-EX team has developed twenty-one operational modes in which the spacecraft will function, with each operational mode consisting of a unique combination of operational onboard hardware (i.e. reaction wheels, radiating antennas, science instrumentation, propulsion, etc.). Examples of these modes can be seen in Figure 3, which highlights the voltage lines and power draw for the three modes related to the FIPEX when operational: FPX1, FPX2, and FPX3. With FPX1 serving as the baseline for FIPEX operations (which also includes hardware such as the Electrical Power System (EPS) board, Command & Data Handling (CDH) board, etc.), FPX2 is identical to FPX1 except with the UHF radio transmitting (therefore constructing a different power-usage state). Likewise, FPX3 is identical to FPX2 except with the X-Band radio transmitting.

Components	Voltage Line [V]	Power [W]	FPX1	FPX2	FPX3
EPS Board		0.34	0.34	0.34	0.34
CDH Board		1.43	1.43	1.43	1.43
GNC Processor	3.3	1.56	1.56	1.56	1.56
GPS		2.03	2.03	2.03	2.03
PROP Electronics + Sensors		0.28	0.28	0.28	0.28
ADCS		5.45	5.45	5.45	5.45
ADCS Peak Power	12	9.23			
UHF Radio (RX)	12	0.37	0.37	0.37	0.37
UHF Radio (TX)		14.98		14.98	14.98
FIPEX	24	7.36	7.36	7.36	7.36
Langmuir Probe	15	0.76	0.76	0.76	0.76
FIPEX Sensor	24	5.89	5.89	5.89	5.89
GlobalStar		6.00			
X-Band Radio		15.75			15.75
PROP Misc. Electronics	10.9	0.03	0.03	0.03	0.03
PROP Valves		8.38			
Battery Heaters		13.00			
Power Totals [W]:			25.51	40.49	56.24

Fig. 3 The FPX1, FPX2, and FPX3 operational modes alongside their power draws and associated voltage lines for the SWARM-EX mission.

These operational modes then serve as the building blocks for thirteen different orbital timelines, or unique combinations of operational modes at varying duty cycles over the course of a single orbit. As illustrated in Figure 4, SWARM-EX has identified four timelines related to SCI experiments, two timelines related to OGNC experiments, five timelines related to commissioning, a Safe Mode timeline, and a Phoenix Mode timeline. Moreover, each orbital timeline is different from the others, and the summation of the duty cycles of all operational modes within a timeline is

<sup>&</sup>lt;sup>2</sup>Phoenix Mode can be thought of as an "ultra-Safe" mode, where only the CDH, EPS, and the UHF receiver are operational and a spacecraft is without attitude control (considered to be "tumbling" immediately following deployment).

always 100%. Each timeline is also specific to the SWARM-EX mission.<sup>3</sup>

					Operat	ional Ork	oits Sumr	mary					
Thi	is table summarizes th	he operational orbits	s (i.e. timelines) defi	ned from the modes	outlined in SYS104-0	ConOps_Timeline_S\	WARM-EX. The cold	ors and duty cycle br	eakdowns correspor	d to the timelines in	SYS104 as well.		SYS104
		*Note* II	you need to change	the names of the ope	rational orbits, do so ir	n this table. If you nee	d to change the nam	es of orbital modes, c	hange these in the "M	odes Breakdown" sh	eet.		
	-Band: Ground s Dayside		v/o X-Band: on is Dayside		-Band: Ground Nightside		//o X-Band: on is Nightside	OGNC Orbi	t w/ X-Band	OGNC Orbit	w/o X-Band		
Name	Duty Cycle	Name	Duty Cycle	Name	Duty Cycle	Name	Duty Cycle	Name	Duty Cycle	Name	Duty Cycle		
FPX1	24%	FPX1	24%	SP1	20%	SP1	20%	SP1	20%	SP1	20%		
	6%	FPX2	6%	GS OPS	6%	SP3	6%	GS OPS	6%	SP3	6%		
SP1	64%	SP1	64%	PROP OPS	1%	PROP OPS	1%	PROP OPS	1%	PROP OPS			
SP2	5%	SP2	5%	SP2	5%	SP2	5%	SP2	5%	SP2	5%		
PROP OPS	1%	PROP OPS	1%	SP1	38%	SP1	38%	SP1	68%	SP1	68%		
				FPX1	30%	FPX1	30%	ļ .					
Safe Mo	ode Orbit	Phoenix I	Mode Orbit	UHF Commi	ssioning Orbit	ADCS Commi	ssioning Orbit	X-Band Comm	issioning Orbit		ommissioning X-Band	Propulsion Co Orbit w/o	ommissionini o X-Band
Name	Duty Cycle	Name	Duty Cycle	Name	Duty Cycle	Name	Duty Cycle	Name	Duty Cycle	Name	Duty Cycle	Name	Duty Cycle
SAFE	20%	PHX	100%	UHF CM1	20%	ADCS CM1	20%	ADCS CM1	20%	SAFE	20%	SAFE	20%
	6%			UHF CM2	6%	ADCS CM2	6%	GS XCM	6%	GS PROP CM	6%		6%
SP4	5%			UHF CM3	5%	ADCS CM3	5%	ADCS CM3	5%	PROP CM	1%	PROP CM	1%
SAFE	69%			UHF CM1	69%	ADCS CM1	69%	ADCS CM1	69%	SP4	5%	SP4	5%
										SAFE	68%	SAFE	68%

Fig. 4 The thirteen orbital timelines defined from the twenty-one operational modes for the SWARM-EX mission.

This modular approach of piecing operational modes into orbital timelines provides a comprehensive understanding of the onboard power usage for the SWARM-EX mission. When linked with the subsequent orbital power generation simulation delineated below, this paradigm allows for full characterization of the SWARM-EX battery SoC.

### V. Orbital Power Generation Simulation

While the SWARM-EX ConOps systematically evaluates onboard power usage, this power draw analysis alone is not a complete picture of the battery SoC. For a given spacecraft to remain power positive throughout an orbit, power draw must be balanced by power generation through appropriately sized and oriented spacecraft solar panels. The layout, size, and general design of the solar panels must meet the system's needs while accounting for eclipses and panel orientation throughout the orbit, including instances where pointing requirements force solar panels to deviate from the Sun. Taking these considerations into account, the SWARM-EX team has conducted an analysis of the orbital power generation by the CubeSat swarm which couples custom pointing profiles and operational orbits with solar panel power generation.

SWARM-EX will gather data on the EIA and ETA through a Flux-Probe-EXperiment (FIPEX) sensor [1] and a Langmuir Probe (LP) [2], respectively, both of which require atomic oxygen flow in the anti-ram direction ( $+\hat{Z}$ ; Figure 1). However, although pointing the instruments in the ram direction enables optimal measurements, this also regularly tilts the spacecraft solar panels away from the sun, thereby resulting in a cosine power loss for power P defined by:

$$P = \eta \cdot \vec{\mathcal{T}} \cdot \vec{A} = \eta \cdot \mathcal{T} A \cos \theta \tag{1}$$

where  $\eta$  is the solar panel efficiency,  $\vec{\mathcal{J}} = \mathcal{J}\hat{S}$  is the solar panel flux vector parallel to the Sun unit vector  $\hat{S}$  for solar constant  $\mathcal{J} \approx 1366 \, [\text{W} \cdot \text{m}^{-2}]$ ,  $\vec{A}$  is the solar panel area vector, and  $\theta$  is the angle between  $\hat{S}$  and  $\vec{A}$ .

This varying cosine loss, along with the high-power usage of the instrument suite ( $\approx$ 14 [W] combined), inhibits the SWARM-EX spacecraft from maintaining a stable power state in a fully ram-aligned attitude configuration. For this reason, a more complex attitude configuration was developed to maximize solar panel power generation while collecting valuable science data based on the maximum angle allowed off ram for each instrument; the SWARM-EX instrument team determined that these angles are 30° and 45° for the FIPEX and the LP, respectively. Consequently, during SCI experiments, the SWARM-EX spacecraft constrain the instrument pointing vectors to a  $\psi = 30^{\circ}$  or  $\lambda = 45^{\circ}$ -cone off ram while simultaneously maximizing the time spent with the solar panels normal to the sun (i.e.  $\vec{A} = A\hat{Z} \parallel \hat{S}$ ).

Likewise, OGNC experiments necessitate an advanced attitude because the onboard control algorithms require accurate and frequent GNSS measurements at close proximities to minimize the risk of conjunctions.<sup>5</sup> The advanced attitude for OGNC orbits therefore restricts a spacecraft's GNSS pointing vector to a  $\phi = 30^{\circ}$ -cone off zenith while

<sup>&</sup>lt;sup>3</sup>The distinction between the ground station being on the dayside vs. the nightside is based on the fact that the FIPEX only takes valuable measurements on the dayside. Likewise, the distinction between "w/" and "w/o" X-Band is due to the lack of need for downlink on the X-Band every orbit.

<sup>&</sup>lt;sup>4</sup>By constraining  $\vec{A} \parallel \hat{S}$ ,  $\theta$  is minimized and P is maximized.

<sup>&</sup>lt;sup>5</sup>The farther off zenith the onboard GNSS patch points, the fewer the number of GNSS satellites in view, not to mention the less favorable geometries of the GNSS constellations that arise (i.e. dilution of precision).

maximizing  $\vec{A} \parallel \vec{S}$ . These attitudes are defined geometrically by the vectors  $\vec{\mathcal{L}}$  and  $\vec{\zeta}$  to which the instrument pointing vectors are aligned.<sup>6</sup>

In order to determine whether these attitude profiles satisfy mission power requirements, an analysis is presented here of the power generated per orbit by the spacecraft solar arrays at minimum and maximum beta angles ( $\beta_{min}$  and  $\beta_{max}$ ) for the various attitude configurations of the SWARM-EX mission.

#### A. $\beta$ Angles

The  $\beta$  angle (or just  $\beta \in [-90^{\circ}, 90^{\circ}]$ ) represents the angle between the satellite orbital plane and the vector to the Sun and serves as an indicator of the percentage of time that a satellite spends in direct sunlight (where it can absorb solar energy). As is detailed in Figure 5, the initial orbital state parameters (defined by state vector **x**) of SWARM-EX produce a  $\beta$  which oscillates between minimum (0°) and maximum ( $\approx 73.5^{\circ}$ ) with a period of around 30 days.

$$\mathbf{x}(t=0) = (a_0, e_0, i_0, \Omega_0, \omega_0, M_0)^{\mathsf{T}} = (6798.14 \text{ [km]}, 0.001, 52^{\circ}, 45^{\circ}, 90^{\circ}, 0^{\circ})^{\mathsf{T}}$$
(2)

for semi-major axis a, eccentricity e, inclination i, right ascension of the ascending node (RAAN)  $\Omega$ , argument of periapsis  $\omega$ , and mean anomaly M.

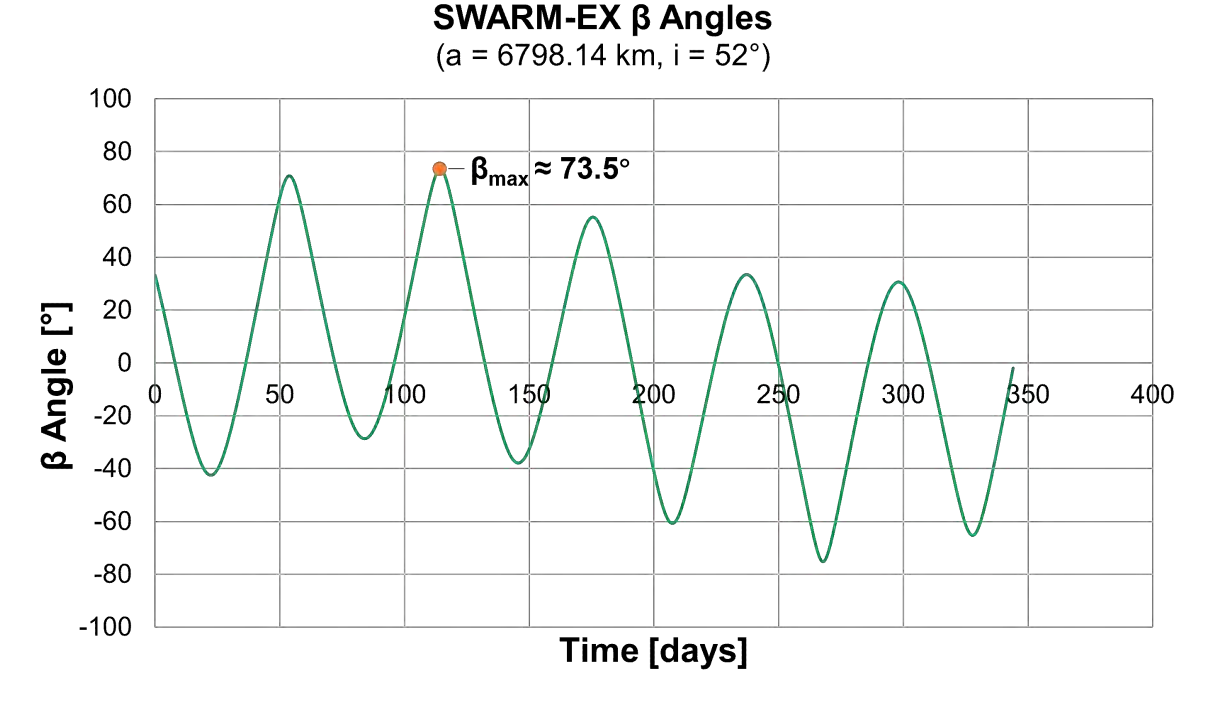


Fig. 5 The various values of  $\beta$  for the SWARM-EX mission, with the peak value of  $\beta_{\text{max}} \approx 73.5^{\circ}$  annotated.

Identifying the time-dependent nature of  $\beta$  illustrates two critical points regarding the SWARM-EX spacecraft power generation:

- 1) A singular orbit can be divided into the dayside (when a spacecraft is in the Sun) and the nightside (when the Earth obscures the Sun and the spacecraft is in eclipse). When  $\beta = \beta_{\text{max}}$ , the SWARM-EX spacecraft are never in eclipse. Table 1 defines the dayside and nightside in terms of their orbital proportions.
- 2) The SWARM-EX spacecraft will always generate more power when  $\beta = \beta_{\text{max}}$  compared to when  $\beta = \beta_{\text{min}}$ . 8 While (2) is a consequence of (1), both distinctions are critical towards understanding the power generation capabilities of the SWARM-EX swarm in its particular orbit. As the duration of the dayside depends strongly on  $\beta$ , the

<sup>&</sup>lt;sup>6</sup>According to the spacecraft body frame detailed in Figure 1, SCI experiments are characterized by  $-\hat{Z} \parallel \vec{\mathcal{L}}$  and OGNC experiments are characterized by  $-\hat{Y} \parallel \vec{\mathcal{L}}$ .

<sup>&</sup>lt;sup>7</sup>This oscillation of  $\beta$  will change for different initial Keplerian elements and is unique to the SWARM-EX orbit.

 $<sup>^8\</sup>beta_{\min}$  and  $\beta_{\max}$  orbits are also commonly referred to as "noon-midnight" and "dawn-dusk orbits," respectively.

Table 1 The dayside and nightside orbital proportions for both  $\beta_{\min}$  and  $\beta_{\max}$  orbits.

β [°]	Dayside	Nightside
0	62%	38%
≈ 73.5	100%	0%

subsequent power analysis analyzes the spacecraft power generation capabilities for both  $\beta_{min}$  and  $\beta_{max}$  to bound the power problem.

## **B. Simulating On-Orbit Power Generation**

Analytical Graphics, Incorporated's Systems Tool Kit (STK) was chosen to simulate the on-orbit power generation of the SWARM-EX spacecraft. Utilizing STK's internal Solar Panel Tool, which calculates the solar power P generated by the satellite model in use for a user-specified amount of time, the generated energy in one orbital period P and average power  $\bar{P}$  are calculated as:

$$\bar{P} = \frac{1}{N} \sum_{i=1}^{N} P_i; \qquad \mathcal{P} = \bar{P} \cdot T \tag{3}$$

where  $P_i$  is the power at each time step i and  $N = \frac{T}{\Delta t}$  is the total number of data points within an orbital period T for time step  $\Delta t$ .

Moreover, due to the differences in solar cell type, solar cell efficiencies, and solar array configuration between the STK satellite model and the SWARM-EX spacecraft,  $P_i$  is further manipulated as:

$$P_{i} = \left(\frac{P_{\text{max}}}{P_{\text{max,STK}}}\right) \left(\frac{\eta}{\eta_{\text{STK}}}\right) \left[\left(\frac{\# \text{ wing cells}}{\# \text{ wing cells STK}}\right) \left(\frac{\# \text{ wing panels}}{\# \text{ wing panels STK}}\right) P_{\text{wings,STK}} + \left(\frac{\# \text{ body cells}}{\# \text{ body cells STK}}\right) \left(\frac{\# \text{ body panels}}{\# \text{ body panels STK}}\right) P_{\text{body,STK}} \right]$$

$$(4)$$

where it is assumed that all wing-mounted and body-mounted cells are respectively co-planar (CP). For SWARM-EX, these parameters assumed into  $P_i$  are defined under AM0 conditions in Table 2 for the pre-existing cubesat\_3u.dae model in STK.9

Table 2 Specifications for the STK CubeSat model file and the SWARM-EX spacecraft used to calculate the subsequent power values.

	P <sub>max</sub> [W]	η	# Wing Cells	# Body Cells	# Wing Arrays	# Body Arrays
STK	1.03	28%	7	7	2	1
SWARM-EX	1.18	32.2%	7	6	4	1

## C. 100% Ram-Pointing Attitude Profile

By harnessing these methods to simulate on-orbit power generation, Figure 6 illustrates the shortcomings of the power generation capabilities of the spacecraft when in the fully ram-aligned attitude profile (denoted "100% Ram-Pointing"), particularly when  $\beta = \beta_{\min}$  and the dayside is shortest. By restricting the SCI instrument suite pointing vector to the ram-direction at  $\beta_{\min}$ , the inevitable power losses due to eclipse are supplemented by the significant cosine losses as the Sun passes overhead; only when the Sun is directly overhead does  $\vec{A} \parallel \vec{S}$  and power generation become maximized. The power losses are less significant at  $\beta_{\max}$  as the Sun looms high in the sky relative to the spacecraft at these times

<sup>&</sup>lt;sup>9</sup>While Figure 1 details only 5 body-mounted solar cells, this analysis is conducted for 6 body-mounted solar cells as per an older design of SWARM-EX. The removal of a body-mounted cell was made due to sizing constraints.

(restricting  $\theta$ ) and there is no time spent in eclipse. Power generation can still be improved, however, as seen when compared to the 100% Sun-Pointing attitude profile.

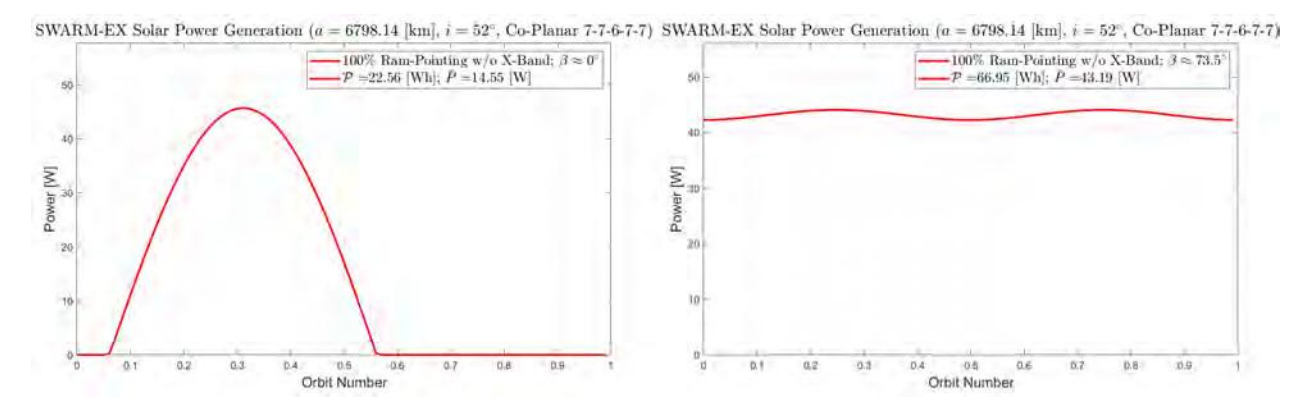


Fig. 6 The summation of the absorbed solar power for the SWARM-EX spacecraft in a 7-7-6-7-7 at (left)  $\beta = \beta_{min}$  and (right)  $\beta = \beta_{max}$  over an entire orbit in the 100% Ram-Pointing attitude mode.

#### D. 100% Sun-Pointing Attitude Profile

Unlike the 100% Ram-Pointing attitude mode, the 100% Sun-Pointing attitude configuration allows maximum power generation by constraining  $\vec{A} \parallel \vec{S}$ ; such restriction eliminates all cosine power losses ( $\theta(t) = 0^{\circ}$ ), as can be seen in Figure 7. This attitude is most pertinent to the Safe Mode orbit timeline, which a spacecraft will transition to in the event that the battery SoC drops below a specified level (i.e. a spacecraft needs to recharge). However, while optimal for power generation, 100% Sun-Pointing inhibits the spacecraft from consistently adhering to the other primary pointing restrictions, such as those imposed on the mission during SCI and OGNC experiments. Consequently, new attitudes must be derived that optimize the balance between power generation and all other mission pointing requirements.

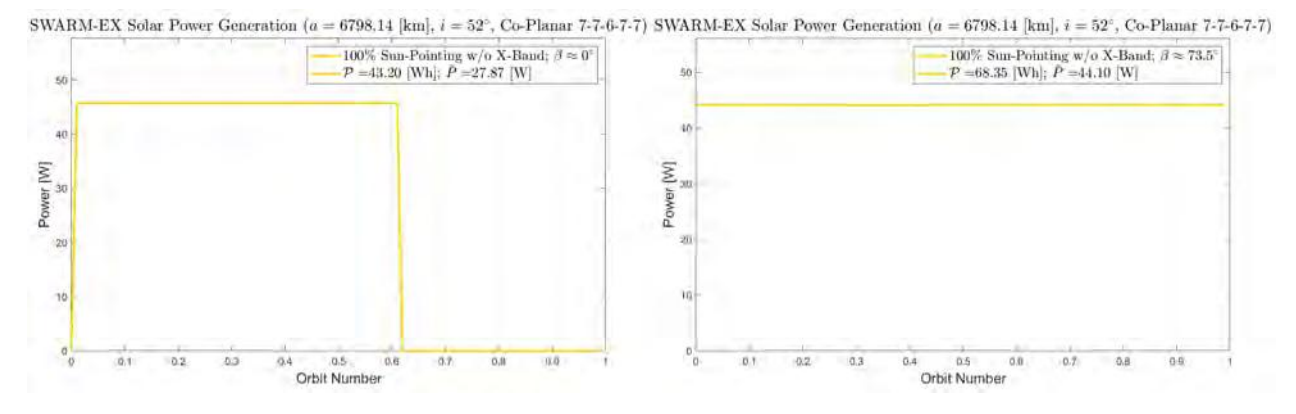


Fig. 7 The summation of the absorbed solar power for the SWARM-EX spacecraft in a 7-7-6-7-7 configuration at (left)  $\beta = \beta_{min}$  and (right)  $\beta = \beta_{max}$  over an entire orbit in the 100% Sun-Pointing attitude mode.

#### E. Advanced Attitude Derivation: $\psi$ -Cone off Ram; Maximize Sun Pointing

While the values calculated from the previous two attitude configurations (100% Ram-Pointing and 100% Sun-Pointing) are helpful for analysis purposes, they cannot serve as the attitude modes pursued during nominal operations when the Science payload (FIPEX and Langmuir Probe) is operational. Although 100% Sun-Pointing will be used during Safe Mode orbits and some parts of commissioning orbits, the realistic operational mode when the Science payload is in use will seek to maximize solar panel power generation while still collecting valuable science data. As such, the more realistic attitude configuration when the Science payload is on will be one that constrains the spacecraft body  $-\hat{Z}$  pointing vector to a 30° or 45°-cone off ram while maximizing the time spent with the solar panel area vector parallel to the Sun pointing vector (i.e.  $\vec{A} = -A\hat{Y} \parallel \vec{S}$ ; Figure 8).

In order to implement this attitude configuration in STK, a custom vector  $\mathscr{L}$  must be defined for the satellite object in the SWARM-EX STK scenario via a VBScript plugin to which the spacecraft body  $-\hat{Z}$ vector must be aligned. 10 The components of this custom vector  $\vec{\mathcal{L}}$ are defined in reference to the Sun-Velocity angle  $\angle SV$ , the spacecraft velocity unit vector  $\hat{v}$ , and the Sun unit vector  $\hat{S}$ , all of which are defined and calculated by STK. Definition of the vector  $\vec{\mathscr{L}}$  is then divided into four cases, each of which is defined based on the value of the allowed angle off ram, which we denote  $\psi$  for the FIPEX and

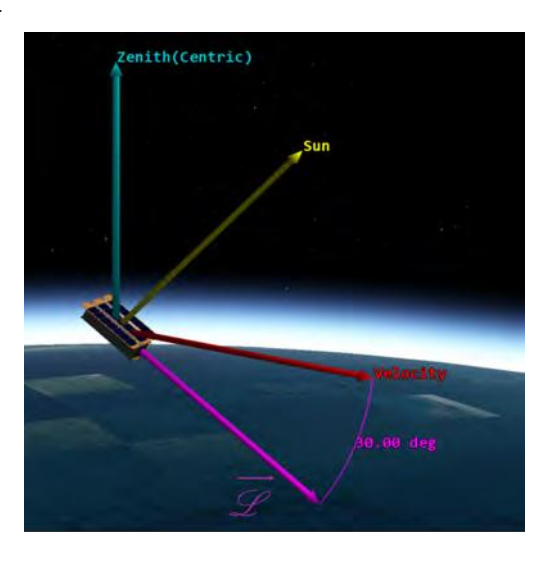


Fig. 8 A screenshot from STK illustrating the  $\psi = 30^{\circ}$ -Cone off Ram pointing mode in a  $\beta_{\min}$  orbit.

 $\lambda$  for the LP. For the analysis following this derivation, we choose to use  $\psi$  only (as it is the more stringent requirement) with  $\psi$  nominally set to 30°; for the purposes of generality, however, the cases are defined in reference to an undefined  $\psi \in [0^{\circ}, 90^{\circ}].^{11}$ 

The four cases defined in Figure 9 are based on the following statements:

- 1) Define some vector of unknown magnitude  $\vec{x} \parallel \hat{S}$ .
- 2) Let \$\vec{x} = \hat{v} + \vec{x} = \hat{v} |\vec{x}| \cdot \hat{S} = \hat{v} x\hat{S}\$.
   3) Recall the Law of Sines: \$\frac{\sin A}{a} = \frac{\sin B}{b}\$ for some angles \$A\$ and \$B\$ of a triangle which face sides \$a\$ and \$b\$, respectively.

With these definitions, all that must be done to define  $\vec{\mathcal{L}}$  is to determine the value of x for each of the four cases.

#### 1. Case I: $0^{\circ} \le m \angle SV < (90^{\circ} - \psi)$

In this case, due to the relationship between  $\angle SV$  and  $\psi$ , the constraint to maximize solar power generation makes the  $\psi$ -cone the limiting factor, such that the spacecraft are locked into an attitude configuration that is  $-\psi^{\circ}$  off ram and yields non-optimal solar power generation according to the value of  $\angle BOS$ , the angle between  $\vec{\mathcal{L}}$  and  $\hat{S}$ . Then, according to the Law of Sines:

$$\frac{\sin\psi}{x} = \frac{\sin\left(180^\circ - \psi - m\angle SV\right)}{|\hat{\nu}|} = \sin\left(180^\circ - \psi - m\angle SV\right) \tag{5}$$

where we have used the fact that the magnitude of a unit vector such as  $|\hat{v}| = 1$ . We can then solve for  $x = x_1$  and, subsequently,  $\vec{\mathcal{L}} = \vec{\mathcal{L}}_{I}$ :

$$x_{\rm I} = \frac{\sin \psi}{\sin \left(180^\circ - \psi - m \angle SV\right)} \tag{6}$$

$$\vec{\mathcal{L}}_{I} = \hat{v} - \left[ \frac{\sin \psi}{\sin \left( 180^{\circ} - \psi - m \angle SV \right)} \right] \hat{S}$$
 (7)

<sup>&</sup>lt;sup>10</sup>Contact the authors for information about the VBScript plugins used for this analysis.

<sup>&</sup>lt;sup>11</sup>In the case where the FIPEX is turned off and only the LP pointing requirement remains,  $\psi$  can simply be replaced by  $\lambda$ .

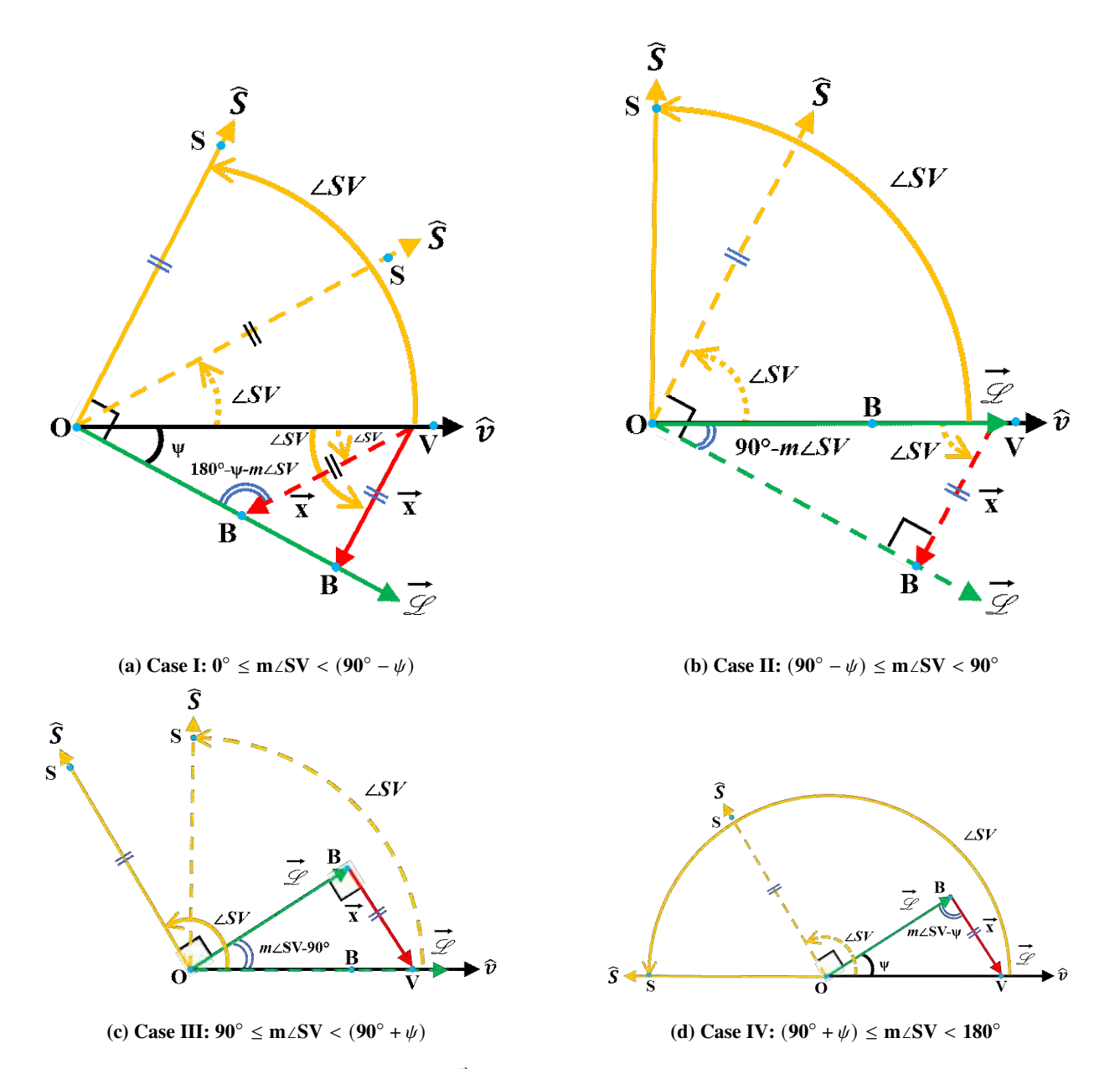


Fig. 9 Depictions of the geometry of  $\vec{\mathcal{L}}$  for the (a) Case I:  $0^{\circ} \le m \angle SV < (90^{\circ} - \psi)$ , (b) Case II:  $(90^{\circ} - \psi) \le m \angle SV < 90^{\circ}$ , (c) Case III:  $90^{\circ} \le m \angle SV < (90^{\circ} + \psi)$ , and (d) Case IV:  $(90^{\circ} + \psi) \le m \angle SV < 180^{\circ}$ .

## 2. Case II: $(90^{\circ} - \psi) \le m \angle SV < 90^{\circ}$

The relationship between  $\angle SV$  and  $\psi$  in this case allows the spacecraft to remain within the  $\psi$ -cone off ram while maximizing solar panel power generation (i.e.  $m\angle BOS = 90^{\circ}$ ) always. Depending on the location of the Sun, the spacecraft will rotate through  $-\psi^{\circ}$  off ram to  $0^{\circ}$  off ram (i.e.  $\vec{\mathcal{L}} \parallel \hat{v}$ ). From this configuration, the Law of Sines produces:

$$\frac{\sin(90^{\circ} - m \angle SV)}{x} = \frac{\sin(90^{\circ})}{|\hat{v}|} = 1$$
 (8)

We can then solve for  $x = x_{II}$  and, subsequently,  $\vec{\mathcal{L}} = \vec{\mathcal{L}}_{II}$ :

$$x_{\rm II} = \sin\left(90^\circ - m\angle SV\right) \tag{9}$$

$$\vec{\mathcal{L}}_{\Pi} = \hat{v} - \left[\sin\left(90^{\circ} - m\angle SV\right)\right]\hat{S}$$
(10)

## 3. Case III: $90^{\circ} \le m \angle SV < (90^{\circ} + \psi)$

Case III is the counterpart to Case II, in that the relationship between  $\angle SV$  and  $\psi$  allows the spacecraft to remain within the  $\psi$ -cone off ram while maximizing solar panel power generation (i.e.  $m \angle BOS = 90^{\circ}$ ) always. Depending on the location of the Sun, the spacecraft will rotate through  $0^{\circ}$  off ram (i.e.  $\vec{\mathcal{L}} \parallel \hat{v}$ ) to  $+\psi^{\circ}$  off ram. From this configuration, the Law of Sines produces:

$$\frac{\sin(m\angle SV - 90^\circ)}{x} = \frac{\sin(90^\circ)}{|\hat{v}|} = 1$$
(11)

We can then solve for  $x = x_{\text{III}}$  and, subsequently,  $\vec{\mathcal{L}} = \vec{\mathcal{L}}_{\text{III}}$ :

$$x_{\text{III}} = \sin\left(m\angle SV - 90^{\circ}\right) \tag{12}$$

$$\mathcal{Z}_{\text{III}} = \hat{v} - \left[\sin\left(m\angle SV - 90^{\circ}\right)\right]\hat{S}$$
(13)

## 4. Case IV: $(90^{\circ} + \psi) \le m \angle SV < 180^{\circ}$

The final case, Case IV, is the counterpart to Case I, as the constraint to maximize solar power generation once again makes the  $\psi$ -cone the limiting factor. The spacecraft are locked into an attitude configuration that is  $+\psi^{\circ}$  off ram and yields non-optimal solar power generation according to the value of  $\angle BOS$ . Then, according to the Law of Sines:

$$\frac{\sin\psi}{x} = \frac{\sin\left(m\angle SV - \psi\right)}{|\hat{v}|} = \sin\left(m\angle SV - \psi\right) \tag{14}$$

We can then solve for  $x = x_{IV}$  and, subsequently,  $\vec{\mathcal{L}} = \vec{\mathcal{L}}_{IV}$ :

$$x_{\text{IV}} = \frac{\sin \psi}{\sin \left(m \angle SV - \psi\right)} \tag{15}$$

$$\vec{\mathcal{L}}_{IV} = \hat{v} - \left[ \frac{\sin \psi}{\sin \left( m \angle SV - \psi \right)} \right] \hat{S}$$
 (16)

The custom vector  $\vec{\mathcal{L}}$  can then be defined by the piecewise function:

$$\vec{\mathcal{L}} = \begin{cases} \hat{v} - \left[\frac{\sin\psi}{\sin(180^\circ - \psi - m\angle SV)}\right] \hat{S}, & 0^\circ \le m\angle SV < (90^\circ - \psi) \\ \hat{v} - \left[\sin\left(90^\circ - m\angle SV\right)\right] \hat{S}, & (90^\circ - \psi) \le m\angle SV < 90^\circ \\ \hat{v} - \left[\sin\left(m\angle SV - 90^\circ\right)\right] \hat{S}, & 90^\circ \le m\angle SV < (90^\circ + \psi) \\ \hat{v} - \left[\frac{\sin\psi}{\sin(m\angle SV - \psi)}\right] \hat{S}, & (90^\circ + \psi) \le m\angle SV < 180^\circ \end{cases}$$

$$(17)$$

#### F. Power Generation: $\psi = 30^{\circ}$ -Cone off Ram; Maximize Sun Pointing

With these new  $\psi = 30^\circ$ -Cone and, by extension,  $\lambda = 45^\circ$ -Cone attitude profiles defined, the solar panel cosine losses are mitigated significantly. As is detailed in Figure 10, the time that  $\theta = 0^\circ$  and  $\hat{A} \cdot \hat{S} = 0$  when  $\beta = \beta_{\min}$  is increased from a single point in the 100% Ram-Pointing attitude to  $\approx 20\%$  of an orbit for the  $\psi = 30^\circ$ -Cone attitude profiles. This allows the spacecraft to generate > 50% more power than when in the 100% Ram-Pointing attitude mode when  $\beta = \beta_{\min}$ . Likewise, the flexibility of the  $\psi = 30^\circ$ -Cone attitude profile fully maximizes power generation when  $\beta = \beta_{\max}$ , identical to the 100% Sun-Pointing attitude profile. These attitude profiles therefore allow peak power generation for a greater segment of time, thereby increasing the overall power generation while still meeting the FIPEX/LP pointing requirements. These marked improvements are characterized in Table 3.

Fig. 10 The summation of the absorbed solar power for the SWARM-EX spacecraft in a 7-7-6-7-7 configuration at (left)  $\beta = \beta_{min}$  and (right)  $\beta = \beta_{max}$  over an entire orbit in the  $\psi = 30^{\circ}$ -Cone attitude mode.

Table 3 The minimum and maximum values of  $\bar{P}$  in [W] for the SWARM-EX spacecraft in a 7-7-6-7-7 configuration at  $\beta=\beta_{min}$  and  $\beta=\beta_{max}$  over an entire orbit in the 100% Ram-Pointing and  $\psi=30^\circ$ -Cone off Ram attitude modes alongside the power generation improvement from the 100% Ram-Pointing to the  $\psi=30^\circ$ -Cone off Ram attitude mode.

β [°]	P̄ <sub>Ram</sub> [W]	$\bar{\mathbf{P}}_{\psi=30^{\circ}}$ [W]	<b>Improvement:</b> Ram $\rightarrow \psi = 30^{\circ}$
0	14.55	21.95	50.9%
≈ 73.5	43.19	44.10	2.1%

## G. Improvements to the $\psi$ -Cone Attitude Profile: 100% SCI Operations

While the  $\psi$ -Cone off Ram attitude mode defined above was a useful first step in determining its value from a power perspective, there are some improvements that need to be made in order for it to serve as the primary attitude profile for SCI experiments. The first of these improvements was made prior to the power analysis presented above: the spacecraft are prevented from rolling over to catch the last minutes of sunlight as the Sun dips below the horizon. At small  $\beta$  angles (i.e.  $\beta < 20^{\circ}$ ), this rolling is excessive, and it would not be feasible for the onboard Attitude Determination & Control System (ADCS) to conduct 180° flips twice every orbit to catch this extra bit of sunlight; not only would this introduce unnecessary complexity to SWARM-EX operations, but it would saturate the reaction wheels of the ADCS far too often, provoking a power spike that nearly negates the extra power generation altogether.

In order to implement this improvement, a second custom vector denoted  $\vec{C}_{\psi}$  to which the spacecraft body  $-\hat{Y}$  vector must be aligned is defined that is parallel with the Sun vector at all times except when  $\beta < 20^{\circ}$  and the Sun-Zenith angle is greater than  $60^{\circ}$ . At this point, the vector is frozen in time, serving as a "shadow" of the Sun vector with which a spacecraft attempts to align its solar panel area vector while maintaining the  $\psi$ -Cone off ram. Mathematically, this can be expressed as:

$$\vec{C}_{\psi} = \begin{cases} \hat{S} + \left[ \frac{\sin(m \angle SZ - 60^{\circ})}{\sin(60^{\circ})} \right] \hat{z}, & \beta < 20^{\circ} \\ \hat{S}, & \text{else} \end{cases}$$
 (18)

Another improvement to this attitude profile is to align the spacecraft body  $-\hat{Z}$  with ram and the solar panel area vector  $(\hat{A} = -A\hat{Y})$  with zenith (i.e.  $\hat{A} = \hat{z}$ ) when the spacecraft are in eclipse. This will not only optimize measurements made by the LP (the FIPEX will not be operational during eclipse), but it will ensure that the spacecraft receive at least one valid GNSS update per orbit.<sup>12</sup>

Finally, the spacecraft must also downlink on the X-Band when they are above  $5^{\circ}$  elevation  $\epsilon$  relative to the ground station. <sup>13</sup> As the X-Band radio is located on the spacecraft's body  $+\hat{Y}$ -side, the attitude of the spacecraft during a

<sup>&</sup>lt;sup>12</sup>While the spacecraft spend no time in eclipse in a  $\beta_{max}$  orbit, such an orbit rarely occurs and a non-zero eclipse time emerges as soon as  $\beta \leq 69^{\circ}$  There is therefore little concern of invalid GNSS measurements during  $\beta_{max}$  orbits.

<sup>&</sup>lt;sup>13</sup>This requirement is set due to the fact that the spacecraft will most likely not be able to close the link when  $\epsilon < +5^{\circ}$  relative to the ground station.

downlink will be characterized by a  $\psi$ -cone off ram while maximizing the time the X-Band pointing vector is aligned with the ground station (GS) pointing vector. This attitude has an identical solution to the one defined previously, except with the Sun vector replaced by the anti-GS pointing vector  $-\hat{G}$  (as the X-Band pointing vector is antiparallel to the solar panel area vector;  $\hat{G} \parallel \hat{Y}$ ) and  $\angle SV$  replaced with  $\angle GV$ .

#### 1. ψ-Cone Conditional Logic

The improvements to the  $\psi$ -Cone attitude profile produce the conditional paths defined in Algorithms 1 and 2.

**Algorithm 1** The logic used for  $\vec{\mathcal{L}}$  to which  $s/c - \hat{Z}$  is aligned.

```
1: if nightside then
               if \epsilon > +5^{\circ} then
 2:
                       -\hat{Z} \leftarrow \vec{\mathcal{Z}}\big|_{-\hat{G}, \angle GV}
 3:
 4:
               else
                       -\hat{Z} \leftarrow \hat{v}
 5:
               end if
 6:
       else if dayside then
 7:
               if \epsilon > +5^{\circ} then
 8:
                       -\hat{Z} \leftarrow \vec{\mathcal{L}}\big|_{-\hat{G}, \angle GV}
 9:
10:
                       -\hat{Z} \leftarrow ec{\mathscr{L}}|_{\hat{S}, \angle SV}
11:
               end if
12:
13: end if
```

**Algorithm 2** The logic used for  $\vec{C}_{\psi}$  to which  $s/c - \hat{Y}$  is aligned.

```
1: if nightside then
             -\hat{Y} \leftarrow \hat{z}
 2:
      else if \beta < 20^{\circ} and m \angle SZ > 60^{\circ} then
              -\hat{Y} \leftarrow \vec{C}_{\psi} \ (\beta < 20^{\circ})
 4:
 5: else
              -\hat{Y} \leftarrow \hat{S}
 6:
      end if
 7:
 8:
 9:
10:
11:
12:
13:
```

#### H. Power Generation: 100% SCI Operations

After incorporating these improvements to the attitude profile, we choose to set the power generation value to zero during a downlink ( $\approx$  6% duty cycle) which occurs during peak power generation to simulate the worst case when the ground station is on the same side of the spacecraft as the Sun (such that the solar panels are forced to turn away from the Sun to expose the X-Band pointing vector towards the ground station). Thus, with the  $\psi$ -cone attitude mode improved, Figure 12 details the power generation for 100% SCI operations with X-Band downlink. As detailed in Table 4, the improvements from the 100% Ram-Pointing to the  $\psi$ -Cone attitude configuration increase even further when X-Band downlink is applied also to the former (Figure 11).

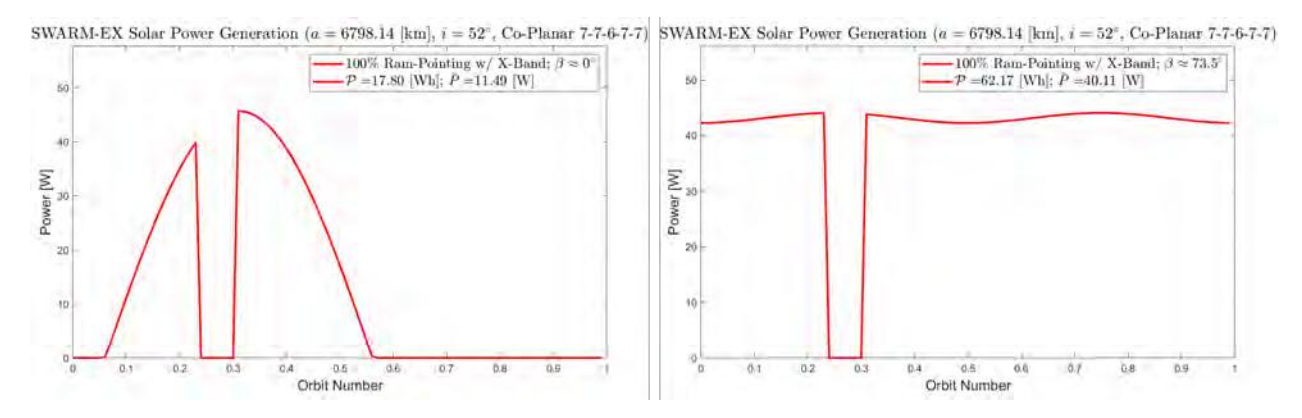


Fig. 11 The summation of the absorbed solar power for the SWARM-EX spacecraft in a 7-7-6-7-7 configuration w/ X-Band downlink at (left)  $\beta = \beta_{min}$  and (right)  $\beta = \beta_{max}$  over an entire orbit in the 100% Ram-Pointing attitude mode.

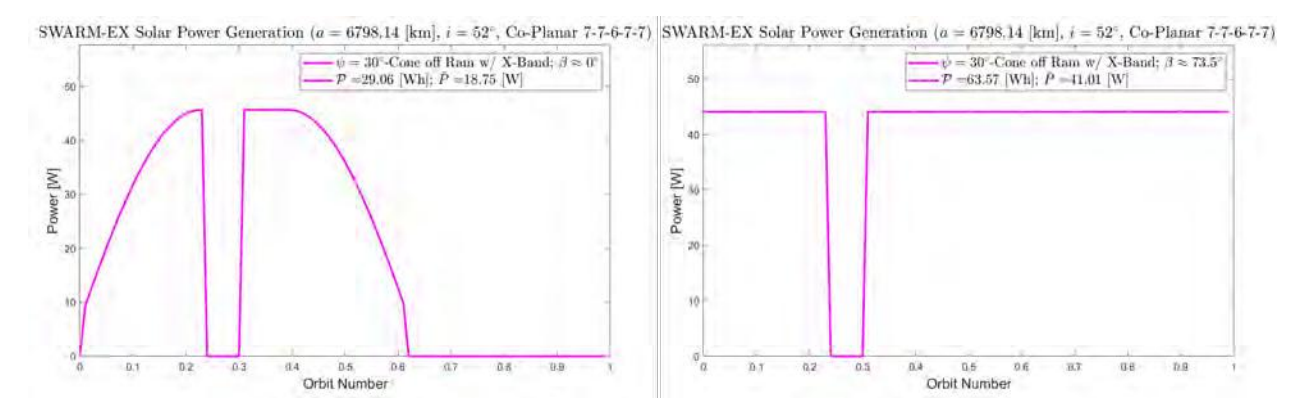


Fig. 12 The summation of the absorbed solar power for the SWARM-EX spacecraft in a 7-7-6-7-7 configuration w/ X-Band downlink at (left)  $\beta = \beta_{min}$  and (right)  $\beta = \beta_{max}$  over an entire orbit in the  $\psi = 30^{\circ}$ -Cone attitude mode.

Table 4 The minimum and maximum values of  $\bar{P}$  in [W] for the SWARM-EX spacecraft in a 7-7-6-7-7 configuration with X-Band downlink at  $\beta=\beta_{min}$  and  $\beta=\beta_{max}$  over an entire orbit in the 100% Ram-Pointing and  $\psi=30^\circ$ -Cone off Ram attitude modes alongside the power generation improvement from the 100% Ram-Pointing attitude profile to the  $\psi=30^\circ$ -Cone off Ram attitude profile.

β [°]	P̄ <sub>Ram</sub> [W]	P̄ <sub>SCI</sub> [W]	<b>Improvement:</b> Ram $\rightarrow \psi = 30^{\circ}$
0	11.49	18.75	63.2%
≈ 73.5	40.11	41.01	2.2%

## I. Advanced Attitude Derivation: $\phi$ -Cone off Zenith; Maximize Sun Pointing

While the  $\psi$ -Cone attitude profile is well suited for SCI experiments, OGNC experiments require a different attitude mode. With the SCI instruments powered off, the  $\psi$ -cone off ram is replaced by a new requirement to have the GNSS patch (located on the spacecraft  $-\hat{Y}$ -face, or in the same plane as the solar array) be within a  $\phi = 30^\circ$ -cone off zenith to obtain accurate and frequent GNSS measurements and mitigate the risk of conjunction during formation flying of the spacecraft when in close proximity ( $\leq 10$  [km] mean along-track separation). As such, we choose to define an advanced attitude for OGNC orbits that restricts a spacecraft's GNSS pointing vector ( $-\hat{Y}$ ) to a  $\phi = 30^\circ$ -cone off zenith while maximizing the time spent with the solar panel area vector parallel to the Sun pointing vector (i.e.  $\vec{A} \parallel \vec{S}$ ; Figure 13).

Just as was done with defining  $\vec{\mathcal{L}}$ , in order to implement this attitude configuration, a custom vector  $\vec{\mathcal{L}}$  must be defined for the satellite object in the SWARM-EX STK scenario via a VBScript plugin. Instead of using the Sun-Velocity angle,  $\vec{\mathcal{L}}$  is defined in reference to the Sun-Zenith angle  $\angle SZ$ , as well as the spacecraft zenith (centric) unit vector  $\hat{z}$  and the Sun unit vector  $\hat{S}$ . Vector definition is divided into two cases, which are defined based on the value of  $m\angle SZ$ . For the analysis following this derivation, this angle  $\phi$  is set to 30°, but for the purposes of generality, the cases are defined in reference to an undefined  $\phi \in [0^{\circ}, 90^{\circ}]$ .

Zenith(Centric)
30.00 deg

Sun

Netocity

Fig. 13 A screenshot from STK illustrating the  $\phi = 30^{\circ}$  off Zenith pointing mode in a  $\beta_{\text{max}}$  orbit.

The two cases defined in Figure 14 are based on the following statements:

<sup>&</sup>lt;sup>14</sup>Contact the authors for information about the VBScript plugins used for this analysis.

- 1) Define some vector of unknown magnitude  $\vec{x} \parallel \hat{S}$ .
- 2) Let  $\vec{\zeta} = \hat{z} + \vec{x} = \hat{z} |\vec{x}| \cdot \hat{S} = \hat{z} x\hat{S}$ .
- 3) Recall the Law of Sines:  $\frac{\sin A}{a} = \frac{\sin B}{b}$  for some angles A and B of a triangle which face sides a and b, respectively.

For brevity, we choose to skip the individual steps required for calculating  $\vec{\zeta}$  for the two cases as was done with  $\vec{\mathcal{L}}$ ; the results are based off the geometry depicted in Figure 14.

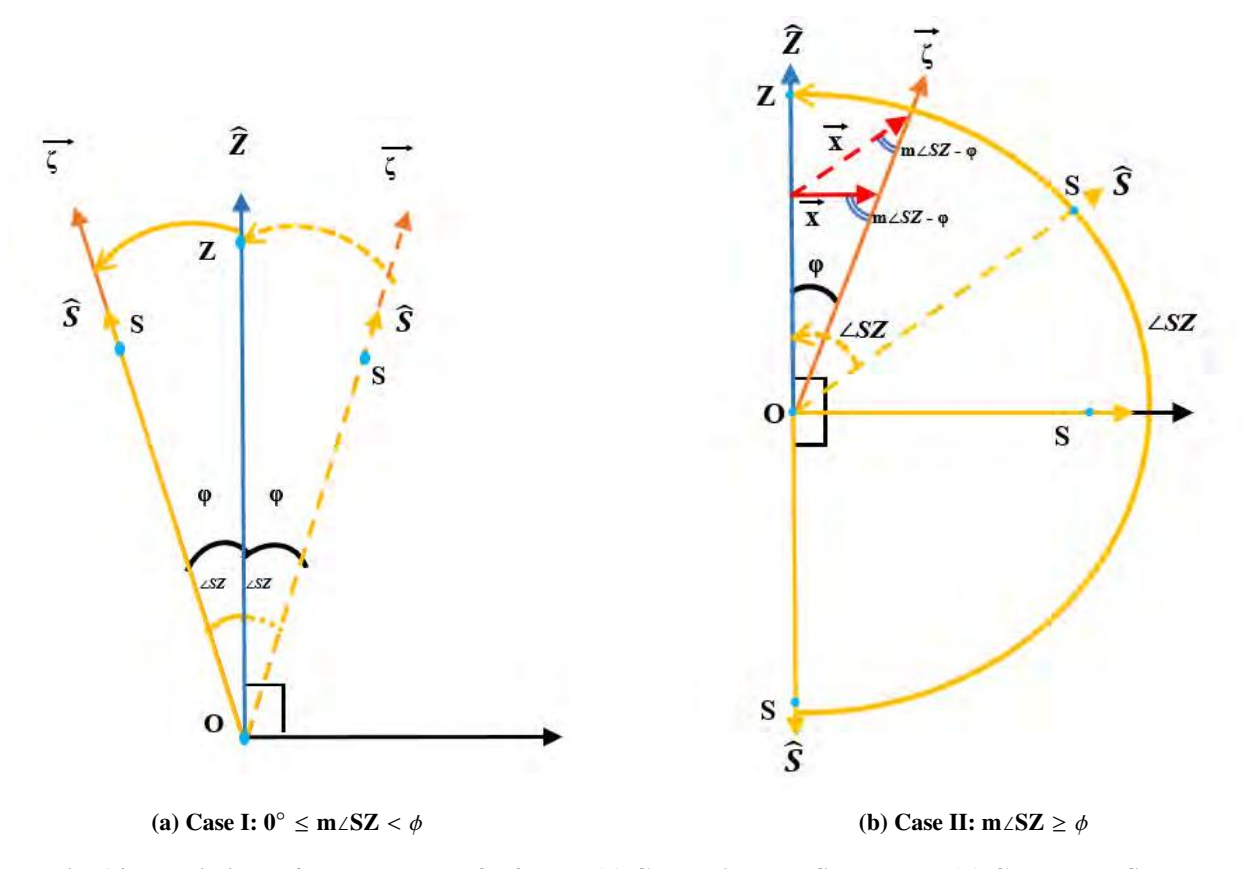


Fig. 14 Depictions of the geometry of  $\zeta$  for the (a) Case I:  $0^{\circ} \leq \text{m} \angle SZ < \phi$  and (b) Case II:  $\text{m} \angle SZ > \phi$ .

$$\vec{\zeta} = \begin{cases} \hat{S}, & 0^{\circ} \le m \angle SZ < \phi \\ \hat{z} + \left[ \frac{\sin(\phi)}{\sin(m \angle SZ - \phi)} \right] \hat{S}, & m \angle SZ \ge \phi \end{cases}$$
 (19)

## J. Power Generation: $\phi = 30^{\circ}$ -Cone off Zenith; Maximize Sun Pointing

Just as with the  $\psi = 30^\circ$ -Cone attitude profile, the  $\phi = 30^\circ$ -Cone attitude configuration similarly mitigates the solar panel cosine losses at  $\beta = \beta_{\min}$ , as is illustrated in Figure 15. Table 5 details how the  $\phi$ -cone **allows the spacecraft to generate** > 50% more power when  $\beta = \beta_{\min}$  than when in the 100% Ram-Pointing attitude mode. While the  $\phi$ -cone unfortunately inhibits the spacecraft from producing more power than when in the 100% Ram-Pointing attitude mode at  $\beta = \beta_{\max}$ , subsequent power analysis reveals that this generation is still sufficient for maintaining a stable battery SoC. Thus, as desired, this attitude profile enables sufficient overall power generation while still meeting the GNSS-Zenith pointing requirement. <sup>15</sup>

<sup>&</sup>lt;sup>15</sup>It should be noted that the power plots when  $\beta = \beta_{min}$  for the  $\psi = 30^{\circ}$ -Cone off Ram and  $\phi = 30^{\circ}$ -Cone off Zenith attitude profiles produce near identical power results. Conceptually, this can be explained by the fact that the attitude profiles are functionally near-equivalent when  $\beta = \beta_{min}$ , as the Solar-Velocity plane and Solar-Zenith plane overlap. This indicates that with these attitude profiles, both SCI and OGNC pointing requirements can be met simultaneously when  $\beta = \beta_{min}$ , a fact which is critical for some of the advanced drag modes incorporated later on in the SWARM-EX mission.

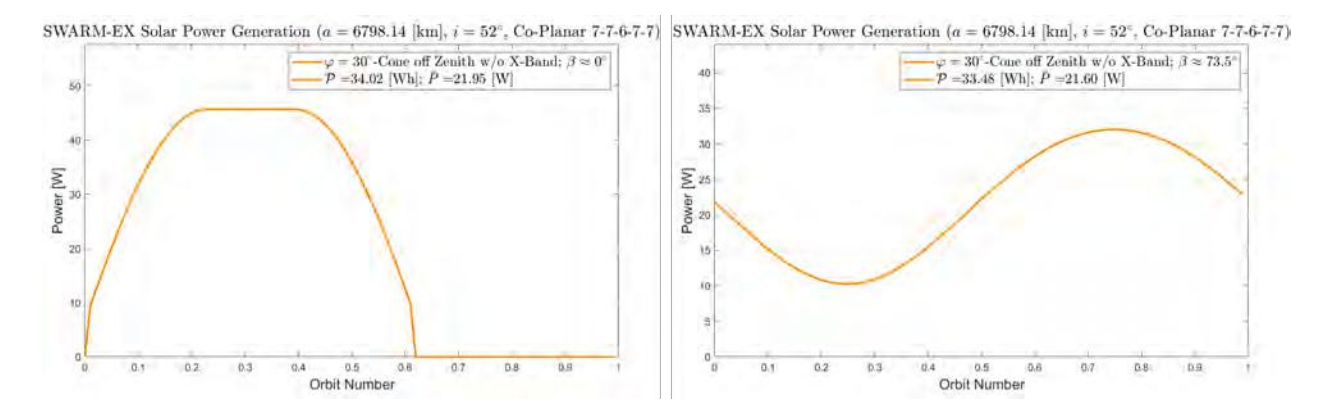


Fig. 15 The summation of the absorbed solar power for the SWARM-EX spacecraft in a 7-7-6-7-7 configuration at (left)  $\beta = \beta_{min}$  and (right)  $\beta = \beta_{max}$  over an entire orbit in the  $\phi = 30^{\circ}$ -Cone attitude mode.

Table 5 The minimum and maximum values of  $\bar{P}$  in [W] for the SWARM-EX spacecraft in a 7-7-6-7-7 configuration at  $\beta=\beta_{min}$  and  $\beta=\beta_{max}$  over an entire orbit in the 100% Ram-Pointing and  $\phi=30^\circ$ -Cone off Zenith attitude modes alongside the power generation improvement from the 100% Ram-Pointing to the  $\phi=30^\circ$ -Cone off Zenith attitude mode.

β [°]	P̄ <sub>Ram</sub> [W]	$\bar{\mathbf{P}}_{\phi=30^{\circ}}$ [W]	<b>Improvement:</b> Ram $\rightarrow \phi = 30^{\circ}$
0	14.55	21.95	50.9%
≈ 73.5	43.19	21.60	-50.0%

## K. Improvements to the $\phi$ -Cone: 100% OGNC Operations

Just as with the  $\psi$ -Cone attitude profile, improvements must be made to the  $\phi$ -Cone attitude configuration for successful OGNC operations. The first improvement is to align the spacecraft body  $-\hat{Z}$  with Ram and the solar panel area vector  $(\hat{A} = -A\hat{Y})$  with zenith (i.e.  $\hat{A} = \hat{z}$ ) when the spacecraft are in eclipse. This will not only optimize measurements made by the LP (the FIPEX will not be operational during eclipse), but it will ensure that the spacecraft receive the most accurate GNSS measurements while in eclipse.

Additionally, the spacecraft must also downlink on the X-Band when they are above  $5^{\circ}$  elevation relative to the ground station. As the X-Band radio is located on the spacecraft's body  $+\hat{Y}$ -side, the attitude of the spacecraft during a downlink will be characterized by a  $\phi$ -cone off zenith while maximizing the time the X-Band pointing vector is aligned with the ground station (GS) pointing vector. This attitude has an identical solution to the one defined previously, except with the Sun vector  $\hat{S}$  replaced by the anti-GS pointing vector  $-\hat{G}$  (as the X-Band pointing vector is antiparallel to the solar panel area vector;  $\hat{G} \parallel \hat{Y}$ ) and  $\angle SZ$  replaced by the supplement of  $\angle GZ$  (i.e.  $180^{\circ} - \angle GZ$ ).

Finally, due to the nature of the GNSS-Zenith pointing constraint, the spacecraft have a degree of freedom in the Tangential-Normal (TN) plane of the familiar Radial-Tangential-Normal (RTN) local frame of the spacecraft. As the LP will often be operational during OGNC experiments, it is recommended that the constraint vector  $\vec{C}_{\phi}$  be set equivalent to  $\hat{v}$ . For maximum power generation, however,  $\vec{C}_{\phi}$  should be set equivalent to  $\hat{z} \times \hat{S}$ . If  $\vec{C}_{\phi}$  is therefore defined as:

$$\vec{C}_{\phi} = \begin{cases} \hat{v}, & \text{LP operational} \\ \hat{z} \times \hat{S}, & \text{LP not operational} \end{cases}$$
 (20)

#### 1. φ-Cone Conditional Logic

The improvements to the  $\phi$ -Cone attitude profile produce the conditional paths defined in algorithms 4 and 5.

<sup>&</sup>lt;sup>16</sup>The difference in power generation between  $\vec{C}_{\phi}$  set to any vector in the TN-plane vs.  $\vec{C}_{\phi} = \hat{z} \times \hat{S}$  is very minimal.

**Algorithm 3** The logic used for  $\vec{\zeta}$  to which s/c  $-\hat{Y}$  is aligned.

```
1: if nightside then
               if \epsilon > +5^{\circ} then
 2:
                      -\hat{Y} \leftarrow \vec{\zeta}\big|_{-\hat{G},(180^{\circ}-\angle GZ)}
 3:
 4:
 5:
               end if
 6:
      else if dayside then
 7:
              if \epsilon > +5^{\circ} then
 8:
                      -\hat{Y} \leftarrow \vec{\zeta}\big|_{-\hat{G},(180^{\circ}-\angle GZ)}
 9:
10:
                      -\hat{Y} \leftarrow \vec{\zeta}|_{\hat{S}, \angle SZ}
11:
               end if
12:
13: end if
```

**Algorithm 4** The logic used for  $\vec{C}_{\phi}$  to which s/c  $-\hat{Z}$  is aligned.

```
1: if LP then
2: -\hat{Z} \leftarrow \vec{C}_{\phi}|_{!LP} = \hat{v}
3: else
4: -\hat{Z} \leftarrow \vec{C}_{\phi}|_{LP} = \hat{z} \times \hat{S}
5: end if
6:
7:
8:
9:
10:
11:
12:
```

## L. Power Generation: 100% OGNC Operations

Once again choosing to set the power generation value to zero during a downlink ( $\approx 6\%$  duty cycle) during peak power generation to simulate the worst case scenario, Figure 16 and Table 6 detail the power results for 100% OGNC operations.

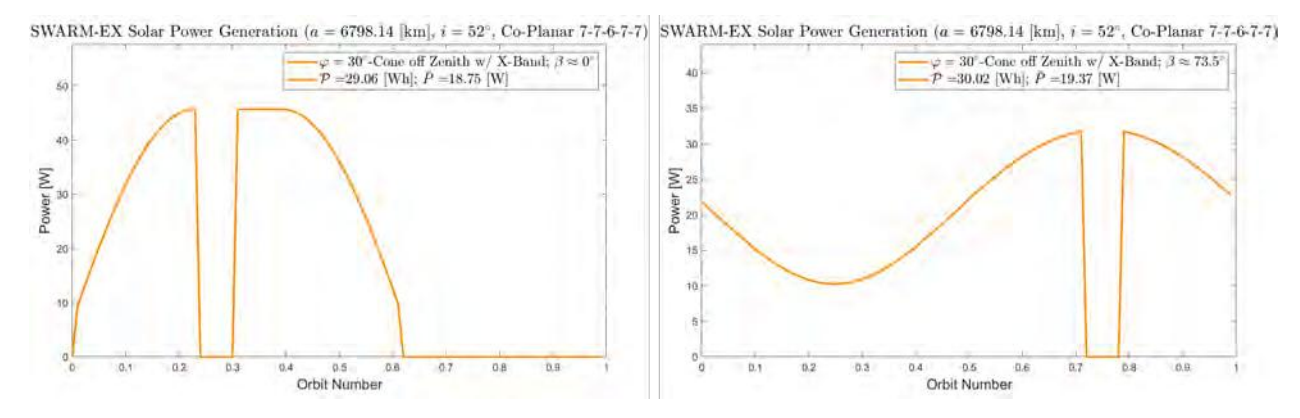


Fig. 16 The summation of the absorbed solar power for the SWARM-EX spacecraft in a 7-7-6-7-7 configuration with X-Band downlink at (left)  $\beta = \beta_{min}$  and (right)  $\beta = \beta_{max}$  over an entire orbit in the  $\phi = 30^{\circ}$ -Cone attitude mode.

Table 6 The minimum and maximum values of  $\bar{P}$  in [W] for the SWARM-EX spacecraft in a 7-7-6-7-7 configuration at  $\beta=\beta_{min}$  and  $\beta=\beta_{max}$  over an entire orbit in the 100% Ram-Pointing and  $\phi=30^\circ$ -Cone off Zenith attitude modes alongside the power generation improvement from the 100% Ram-Pointing to the  $\phi=30^\circ$ -Cone off Zenith attitude mode.

β [°]	P̄ <sub>Ram</sub> [W]	Pognc [W]	<b>Improvement:</b> Ram $\rightarrow \phi = 30^{\circ}$
0	11.49	18.75	63.2%
≈ 73.5	40.11	19.37	-51.7%

## M. Power Results Summary

Table 7 summarizes the power values across all the attitude modes aforementioned.

Table 7 The minimum and maximum values of  $\bar{P}$  in [W] and accompanying parameters for the SWARM-EX spacecraft in a 7-7-6-7-7 configuration at  $\beta=\beta_{min}$  and  $\beta=\beta_{max}$  over an entire orbit in the 100% Ram-Pointing w/o X-Band downlink, 100% Sun-Pointing,  $\psi=30^\circ$ -Cone off Ram,  $\phi=30^\circ$ -Cone off Zenith, 100% SCI operations ( $\psi$ -cone, SP, GS), and 100% OGNC operations ( $\phi$ -cone, SP, GS) attitude modes.

	Power [W]						
β [°]	$\bar{\mathbf{P}}_{\mathbf{Ram}}$	$ar{\mathbf{P}}_{\mathbf{Sun}}$	$\bar{\mathbf{P}}_{\psi=30^{\circ}}$	$ar{\mathbf{P}_{\phi=30^{\circ}}}$	$ar{\mathbf{P}}_{\mathbf{SCI}}$	Pognc	
0	14.55	27.87	21.95	21.95	18.75	18.75	
≈ 73.5	43.19	44.10	44.10	21.60	41.01	19.37	

## N. SCI Orbits: Mapping to ConOps Timelines and Modes

While the power calculations from the simulations of 100% SCI/OGNC operations provide a more exact power estimate of the spacecraft, neither SCI nor OGNC orbital timelines will have conerestricted attitudes for 100% of the time. Rather, actual on-orbit operations will be characterized by an aggregate of different attitude modes depending on the operational mode. For example, Figure 17 details the breakdown for the "SCI Orbit w/ X-Band: Ground Station is Dayside" orbit, which contains various attitudes:

- FPX1:  $\psi = 30^{\circ}$ -Cone off Ram; Maximize Sun-Pointing
- FPX3:  $\psi = 30^{\circ}$ -Cone off Ram; Maximize GS-Pointing
- SP1/2:  $\lambda = 45^{\circ}$ -Cone off Ram; Maximize Sun-Pointing
- PROP OPS: 100% Ram-Pointing

Unfortunately, it is difficult to incorporate duty cycles and time knowledge into STK, as plugin scripts are calculated at each time step and do not retain information from one iteration to the next. While this should not be an issue for implementation into the SWARM-EX flight software with GNSS time knowledge, the power generated for

SCI Orbit w/ X-Band: Ground Station is Dayside				
Name	Duty Cycle			
FPX1	24%			
FPX3	6%			
SP1	64%			
SP2	5%			
PROP OPS	1%			

Fig. 17 The operational modes and accompanying duty cycles for the "SCI Orbit w/X-Band: Ground Station is Dayside" orbital timeline.

the orbits can be calculated by taking an aggregate of multiple power simulations for each attitude. From here, these power-generation values can be linked with the predefined orbital timelines in the SWARM-EX Power Budget to fully characterize the spacecraft battery SoC.

## VI. Differential Drag Analysis

In order to minimize the amount of propulsion expended, SWARM-EX intends to utilize the appreciable orbital effects of atmospheric drag in LEO for maneuvers and formation reconfiguration. By altering the effective surface area perpendicular to the direction of motion of one of the spacecraft through a change in that spacecraft's attitude, the effects of atmospheric drag on spacecraft acceleration can be controlled. For a swarm of small satellites, this management of spacecraft drag characteristics can be used to produce a difference in the acceleration between the spacecraft in the swarm. Setting one spacecraft in a low-drag (LD) configuration with another in a high-drag (HD) configuration, this acceleration difference due to drag between spacecraft yields "differential drag" that can vary the mean along-track separation between the CubeSats.

Increasing and decreasing the mean along-track separation between the SWARM-EX spacecraft (referred to as "expansion" and "contraction" of the swarm) is planned to occur during some of the mission's SCI experiments in an effort to evaluate the evolution of the EIA/ETA over varying spatial and temporal regions. Consequently, the SWARM-EX spacecraft are required to maintain the  $\psi$ -Cone off Ram attitude profile during these differential drag maneuvers for at least one of the three spacecraft in the swarm. For efficient expansion/contraction, the SWARM-EX team has identified that the differential ballistic coefficient  $\Delta B$  between the spacecraft must be at least 200%, where B and B are defined as:

$$B = \frac{C_D A}{m}; \qquad \Delta B = \left| \frac{B_{\text{HD}} - B_{\text{LD}}}{B_{\text{LD}}} \right| \tag{21}$$

where  $C_D$  is the empirically-determined drag coefficient, A is the cross-sectional area, and m is the spacecraft mass.

Noting this requirement, the SWARM-EX team plans to utilize the Safe Mode orbit timeline for the high-drag attitude as it is defined by the 100% Sun-Pointing attitude profile and provides the best opportunities to maximize  $\Delta B$ . Table 8 then illustrates that with these definitions,  $\Delta B$  at both extremes of  $\beta$  is at least 200%, thereby indicating that the  $\psi$ -Cone attitude profile also satisfies the requirements imposed by differential drag.

Table 8  $\Delta B_{\text{avg}}$  over an orbital period at  $\beta_{\text{min}}$  and  $\beta_{\text{max}}$  during the differential drag expansions/contractions of SWARM-EX.

	$\beta_1$	min	$\beta_{ ext{max}}$	
	Low Drag High Drag		Low Drag	High Drag
Operational Orbit:	SCI	Safe Mode	SCI	Safe Mode
Average ΔB:	354.3%		200%	

# VII. SWARM-EX Power Budget: A Spacecraft Battery State of Charge Simulation Tool

With knowledge of how the spacecraft use and generate power during each orbital timeline, the spacecraft power stability can be modeled using the SWARM-EX Power Budget, an automated, user-interactive spreadsheet which simulates the battery SoC for three orbital timelines and parameters of the user's choosing (Figure 18). Configurable items include:

- Orbital timelines for orbits 1, 2, and 3.
- $\beta$  angle.
- Number of body-mounted solar panels.
- Number of wing-mounted solar panels.
- Number of solar cells per wing panel.
- Number of solar cells per body panel.
- Battery capacity [Watt-Hours] and yearly degradation.
- Solar cell temperature, peak power, efficiency, yearly degradation, and temperature gradients.
- Beginning of Life (BOL)/End of Life (EOL) battery/solar cell parameters.
- An additional contingency.

Following the definitions of these parameters, the power budget takes in the power draw and power generated at each time step (1% of an orbit) to calculate the corresponding battery  $SoC \in [0\%, 100\%]$  as:

$$SoC = \frac{\mathcal{P}_{generated} - \mathcal{P}_{used}}{\mathcal{P}_{max,battery}} \times 100\%$$
 (22)

From the expression for the SoC, it can be seen that if  $\mathcal{P}_{used} > \mathcal{P}_{generated}$ , a spacecraft is forced to draw energy from the battery. While this is an expected phenomenon, it is critical that the SoC returns to 100% after a few orbits to indicate stability in the battery power state; a steady decrease in the SoC would eventually deplete the battery and yield an inoperable spacecraft. The power budget therefore also calculates the time until battery depletion based on the slope of the SoC.

Serving as the culmination of the power analysis, the power budget indicates that **the SWARM-EX spacecraft will remain power-positive during all thirteen orbital timelines**. This not only validates the efficacy of the  $\psi$ -cone and  $\phi$ -cone attitude profiles, but also assures the team that the mission is well-positioned for success from the perspective of power.



Fig. 18 A screenshot from the SWARM-EX power budget illustrating its capability to simulate the battery SoC for three orbital timelines (three Safe Mode orbits at  $\beta = \beta_{min}$  are shown) of the user's choosing, allow the input of various parameters, and identify the stability of the spacecraft power state.

#### VIII. CIRBE CubeSat

With an established environment of collaboration between Cube-Sat development teams at CU Boulder, the SWARM-EX team continually seeks to make use of the expertise of other CubeSat missions at CU throughout the satellite design process. One such project is the Colorado Inner Radiation Belt Experiment (CIRBE), which provided the impetus for some of the techniques utilized in the aforementioned SWARM-EX power analysis. To illustrate the portability of these methods, this section outlines the power summary for CIRBE as a supplemental case study.

The objective of CIRBE is to understand the formation of the inner radiation belt electrons <sup>17</sup> and to determine the source, intensity, and dynamic variations of these electrons using a novel instrument fitted into a 3U CubeSat in a 97°, 500 [km] polar orbit. This cutting-edge science instrument is the Relativistic Electron Proton Telescope integrated little experiment-2 (REPTile-2), which is being designed and built at the Laboratory for Atmospheric and Space Physics (LASP) in Boulder, CO. The spacecraft bus is a third generation XB1 spacecraft designed and built by Blue Canyon Technologies (BCT) and is designed for LEO with two deployable solar panels, a deployable UHF monopole antenna, an S-Band transmitter, and a GPS receiver (Figure 19).

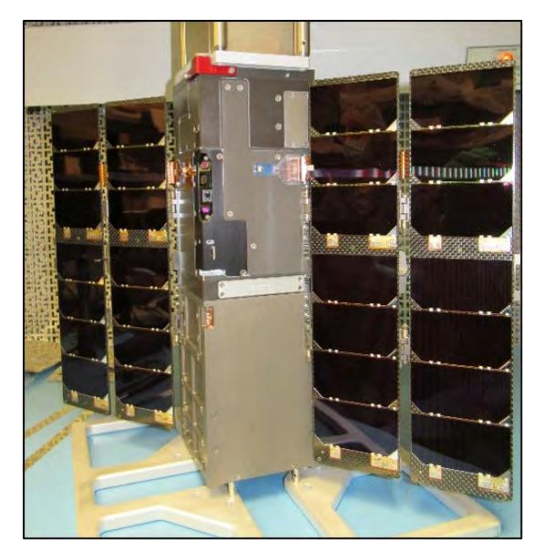


Fig. 19 The CIRBE CubeSat with solar panels attached to ground support frames.

The ConOps for CIRBE is relatively simple compared to that of SWARM-EX, with the flight operations for CIRBE consisting of three nominal attitude modes: Science, Downlink, and Sun-Safe. The Science and Sun-Safe attitude modes both have a primary rule to keep the spacecraft solar panels Sun-pointed, while the Science attitude mode has a secondary rule to keep the REPTile-2 pointing vector (located on the front-facing 1U face) perpendicular to the local magnetic field vector. This nominal Science mode is referred to as CIRBE's "Rotisserie" mode as it results in the spacecraft spinning slowly about the solar panel area vector (Figure 20). The Downlink attitude mode's primary rule is to point the S-Band antenna (located on the 1U face opposite the instrument pointing vector) directly toward the ground station with a secondary rule to maximize solar array alignment with the Sun.

Analogous to that of SWARM-EX, CIRBE's power budget was analyzed through a worst-case-orbit approach by

<sup>&</sup>lt;sup>17</sup>These electrons have energies that range from hundreds of keV to a few MeV.

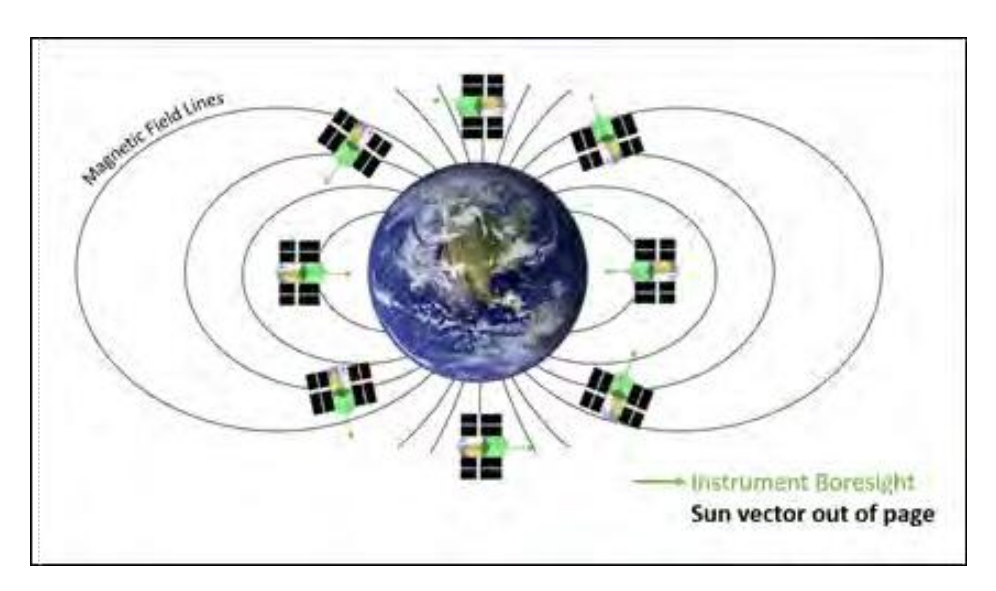


Fig. 20 A depiction of CIRBE's "Rotisserie" mode to remain Sun-pointed with the instrument pointing vector perpendicular to the local magnetic field for nominal Science operations.

comparing the solar panel power generation to the total system power draw over the course of one full 94-minute orbit. The worst-case orbit from a power perspective occurs when  $\beta = \beta_{min} = 0^{\circ}$ , which has an eclipse period of  $\approx 36$  minutes. This worst-case orbit also includes a 5-minute ground station pass on the dayside; for the sake of a conservative power analysis, the spacecraft solar panels receive no power during the pass. The worst-case orbit analysis, CIRBE generates solar power for 53 minutes per 94-minute orbit, with 41 minutes spent using battery power in eclipse and during a ground station pass. The total system power draw was calculated in a spreadsheet by using the expected power draw of each subsystem in Table 9, including the XB1 subsystems and the REPTile-2 payload. The REPTile-2 payload and some XB1 subsystems such as the reaction wheels, flight computer, and UHF receiver were assumed to have a 100% duty cycle; other XB1 subsystems such as the UHF transmitter, heaters, and GPS receiver possess duty cycles below 100%.

Table 9 The subsystems included in the CIRBE power analysis.

Spacecraft Bus	Communications	Payload	Battery
Flight Computer	UHF Receiver	Processor Board	Battery Charging
Star Tracker	S-Band Transmitter	Power Board	-
Reaction Wheels	UHF Transmitter	ADC Board	-
Torque Rods	-	Charge Sensitive Amplifiers	-
GPS Receiver	-	-	-
Battery Heater	-	-	-
Bus Heater	-	-	-

To balance the power draw of all operations in the 94-minute orbit and verify that the system successfully passes the worst-case orbit analysis, the solar panels of CIRBE must provide enough power generation in the 53 minutes of sunlight. The results of CIRBE's worst-case-orbit calculations are shown in Table 10 and illustrate that the spacecraft requires 25.6 [W] of solar array power in order to balance the operational draw. Since CIRBE's two bifold solar panels generate 28.4 [W] of power, the resulting 10.8% margin in this conservative worst-case orbit analysis provides the CIRBE team with confidence that the spacecraft will remain power-positive throughout its operational lifetime.

<sup>&</sup>lt;sup>18</sup>During actual on-orbit operations, the spacecraft will roll about the antenna vector to receive limited solar power.

Table 10 The results of CIRBE's worst-case-orbit power analysis.

Required Solar Array Power	25.6 [W]
System Solar Array Power	28.4 [W]
System Power Margin	10.8%
Battery Worst Case SoC	85.93%

#### IX. Conclusion

Acknowledging the complexity of the mission's technical objectives, the SWARM-EX team has harnessed the expertise of previous CU CubeSat missions like CIRBE to develop a process for analyzing a spacecraft's on-orbit power stability that combines a ConOps established using operational modes and orbital timelines, advanced attitude profiles simulated in STK, and an automated SoC simulation tool serving as the power budget. The modular approach to the ConOps classifies all possible on-orbit power-draw states based on projected mission operations for the SWARM-EX mission. The attitude profiles developed are derived geometrically to satisfy the various pointing requirements during SCI and OGNC experiments while simultaneously maximizing power generation. When these profiles are applied to the SWARM-EX orbit, the intersection of the ConOps with the power values generated by STK in these attitude profiles allows the power budget to readily illuminate critical power issues, thereby facilitating improved comprehension of spacecraft performance during each mission phase.

As small satellite projects continue to push scientific and technical boundaries, coordinated processes like these will become more necessary for successful operations. The approach described here has allowed the SWARM-EX team to systematically mitigate the risk of not sustaining power-positive operations; the team is now confident that the spacecraft swarm will have enough power to execute the mission's objectives. Therefore, the SWARM-EX team aims to have these techniques serve as a specific case from which more advanced planning processes can be derived, some of which may proliferate to other small satellite projects throughout the field.

#### References

- [1] Eberhart, L. S. S. A. B. T. F. S., M., "Measurement of atomic oxygen in the middle atmosphere using solid electrolyte sensors and catalytic probes," *Atmospheric Measurement Techniques*, Vol. 8, No. 9, 2015, pp. 3701–3714.
- [2] Fish, S. C. M. C. G. B. A. N. T. G. J. A. I. P. M. W. R. A. D. A. M. B. B. B. K. B. S. B. R. B. B. C. J. D. K. F. C. M., C. S., "Design, development, implementation, and on-orbit performance of the dynamic ionosphere cubesat experiment mission," *Space Science Reviews*, Vol. 181, No. 1-4, 2014, pp. 61–120. https://doi.org/https://doi.org/10.1007/s11214-014-0034-x.